Journal of Computers Vol. 28, No. 1, 2017, pp. 261-271
doi:10.3966/199115592017022801020

The Obstacle Avoidance Systems on the Wheeled Mobile Robots with Ultrasonic Sensors

Ter-Feng Wu[1*], Pu-Sheng Tsai[2], Nien-Tsu Hu[3], and Jen-Yang Chen[4]

[1] Department of Electrical Engineering, National Ilan University
Yilan 260, Taiwan, ROC
tfwu@niu.edu.tw

[2] Department of Electronic Engineering, China University of Science and Technology
Taipei 115, Taiwan, ROC
tps@ee2.cust.edu.tw

[3] Chemical Systems Research Division, National Chung-Shan Institute of Science and Technology
Taoyuan 325, Taiwan, ROC
nientsu.hu@gmail.com

[4] Department of Electronic Engineering, Ming Chuan University
Taoyuan 333, Taiwan, ROC
jychen@mail.mcu.edu.tw

Received 18 June 2015; Revised 19 February 2016; Accepted 27 December 2016

Abstract. The purpose of this study is to combine ultrasonic and CMOS image sensors In this study, CMOS image sensor was used to deal with small obstacles and to retrieve image information in front of the robot. In this work, ultrasonic sensors are adopted to implement a real-time obstacle avoidance system for wheeled robots, so that the robot can continually detect surroundings, avoid obstacles, and move toward the target area. Secondly, six ultrasound sensors installed on the wheeled robot were utilized to detect large obstacles and to obtain distance information between the robot and the obstacle. The PD controller was used in the wall-following method to achieve the optimized path design. Experimental results verified that ultrasonic sensors of the obstacle avoidance system on the wheeled robot, with ATMega162 embedded microcontroller as the core of the system, can indeed help avoid obstacles and reach the established target area.

Keywords: obstacle avoidance strategy, ultrasonic sensor, wall-following algorithm, wheeled mobile robot

1 Introduction

Path planning, obstacle avoidance, and tracking trajectory control have become widely discussed research topics in the field of wheeled robots navigation. Robot paths are planned include two major areas: environment model-based algorithm and sensor-based algorithm. In an environment model-based system, the primary task is to construct a method of describing the working environment and the distribution model of obstacles. The most frequently cited methods include Potential Fields Method, Cell Decomposition Method, Analytical Description of Curves and Vertices Search Method [1-4]. The sensor-based system is utilized an unknown or changing environment, to perform real-time obstacle avoidance and real-time path planning functions. The sensing elements that are most commonly found in the literature include infrared and ultrasound, CCD camera or CMOS image sensors, laser light pens, global positioning

* Corresponding Author

systems (GPS), etc. Early approaches involved affixing easily reflective stickers on the ground or installing induction pipelines underground. Established routes were navigated by infrared detection [5]. However, this approach cannot avoid an object's sudden appearance. Since ultrasonic sensors are easily obtained and inexpensive, and they are effective in distance measurement, obstacle avoidance, or even on-street parking applications. Ultrasonic sensors have for a long time been major components of devices for detecting obstacles and exploration the unknown environment. Jiang et al. [6] utilized six ultrasonic sensors to capture relative information about of ambient wheeled robots and to identify a parking space for automatic parking. In addition, the wall-following algorithm is regarded as one of the most common and most practical obstacle avoidance algorithms. Adopting ultrasonic sensors to achieve the obstacle avoidance strategy of wall-following algorithms have become the research subject of many scholars. In 1995, Yuta and Ando [7] installed ultrasonic sensors on the front of a robot and in various locations on the left and right hand sides. Successful wall-following depends entirely on ultrasonic distance information. In 1992, Huang and Lee [8] developed two obstacle avoidance strategies – the Heuristic mode (H mode) and the Track mode (T mode) strategies. The T-mode strategy is an algorithm that allows the robot to maintain a safe distance from an obstacle while moving forward along one of its edges. In this paper, the wall-following method has been demonstrated to have the characteristics of shortest distance of obstacle avoidance path. A follow-up article [9] revealed that the fuzzy inference method for implementing the H mode and the T mode strategies was viable. Further, ranging data from multiple ultrasonic sensors combined to create a map of the surrounding environment or to establish a model of the shape of the surface of an obstacle is another important research topic [10-11].

This investigation combines the ATMega162embedded microcontroller as the core of the system with ultrasonic sensors to detect large obstacles in the environment, and used the wall-following method to avoid obstacles. In our study tried to use the distance information of the four ultrasonic sensors to perform obstacle avoidance strategy of the wall-following method. The breakdown of this bottleneck will solidify the research potential of various small robots follow.

2 Obstacle Avoidance System of Wheeled Robot

The wheeled mobile robot that was utilized in this study is composed of four rigid bodies. The main body is supported respectively by a platform, left and right two fixed wheels, and a castor wheel to support the robot weight. For the sensing element, Ultrasonic sensors were installed on the left front, right front, and the left-and right-hand sides of the robot. Four SRF05 ultrasonic sensors, produced by Devantech Company, were used to detect the presence of large obstacles. Those sensors obtained the corresponding relationship between the robot and the obstacle to implement the wall-following avoidance strategy to move around the obstacle toward the goal. The wheeled mobile robot's power source is provided by two servo motors fixed in the left and right wheels, which were used to control the forward motion, backward motion, left and right turns, and other related actions, of the robot. A TDCM3 electronic compass, produced by Topteam Technology, was installed on the actual vehicle to obtain the azimuth angle between the robot and the north. Fig. 1 presents the body of the wheeled robot and Fig. 2 shows the overall block diagram of the ultrasonic-based obstacle avoidance system.

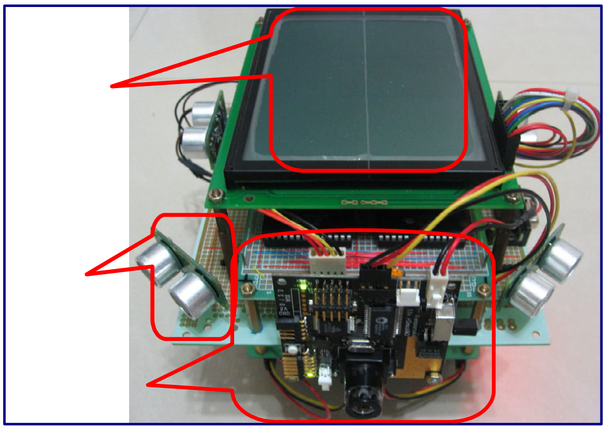

Fig. 1. The Body of wheeled mobile robot

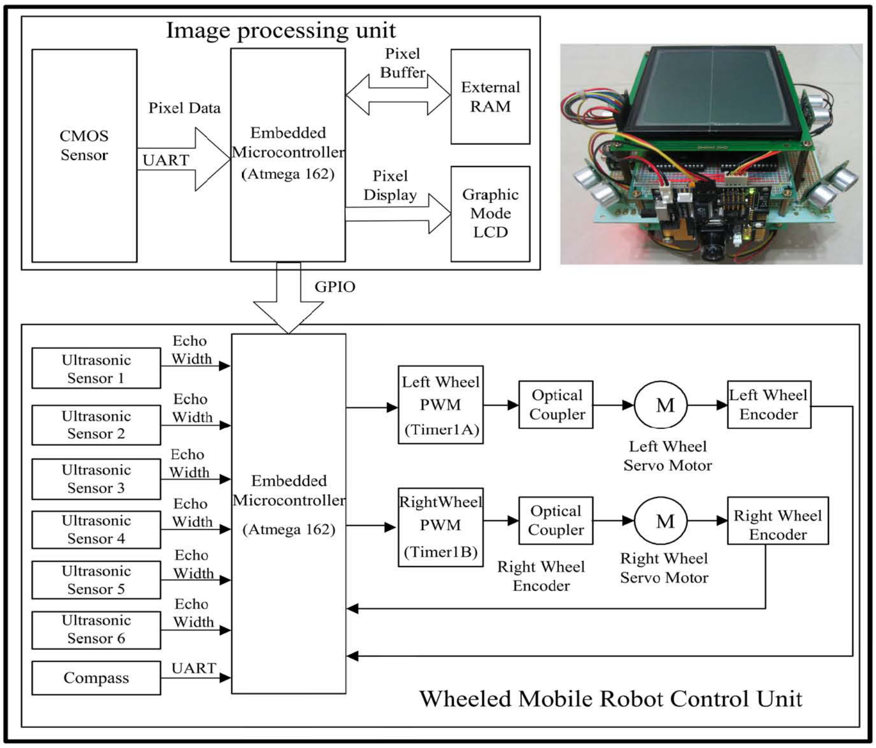

Fig. 2. System block diagram

2.1 SRF05 Ultrasonic Sensors

The ultrasonic sensors that are used in the proposed system are SRF05 modules, which are produced by Devantech and shown in Fig. 3. Their measurement range is 1 cm to 4 m, with superior measurement performance. The relevant control timing diagram can be observed in Fig. 4. First, the embedded microcontroller that was installed in the robot control board was used to send a 10 μs high-state pulse to the trigger input pin of SRF05 ultrasonic module, making its internal oscillator generate and emit eight cycles of 40KHz ultrasonic signal and the Echo output pin convert to a high-state level. The ultrasonic signal hits the obstacles and rebounds to the SRF05 module, which reduces the level of the Echo output pin to a low. Since the Echo signal maintains the width of the high level proportional to the time of the ultrasound transmit and bounce. As so the use of the pulse width to determine the distance between ultrasound module and the obstacle is feasible.

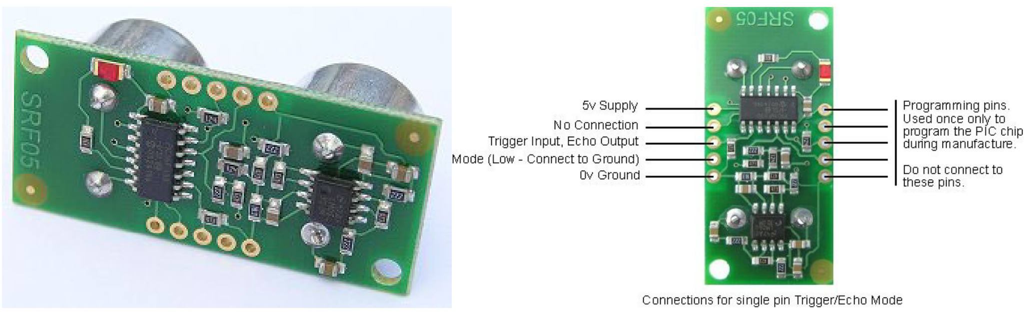

Fig. 3. SRF05 ultrasonic modules

According to the specifications that were provided by the vendor and the experimental results, the distance (cm) between ultrasound sensor and obstacle is the duration of the Echo high-state pulse (μs) multiplied by a scale factor of $1/60\,(cm/\mu s)$. The timing diagram in Fig. 4 shows the Echo high-state pulse width from $100\mu s \sim 25ms$, so the distance that could be measured by the SRF05 ultrasonic modules is

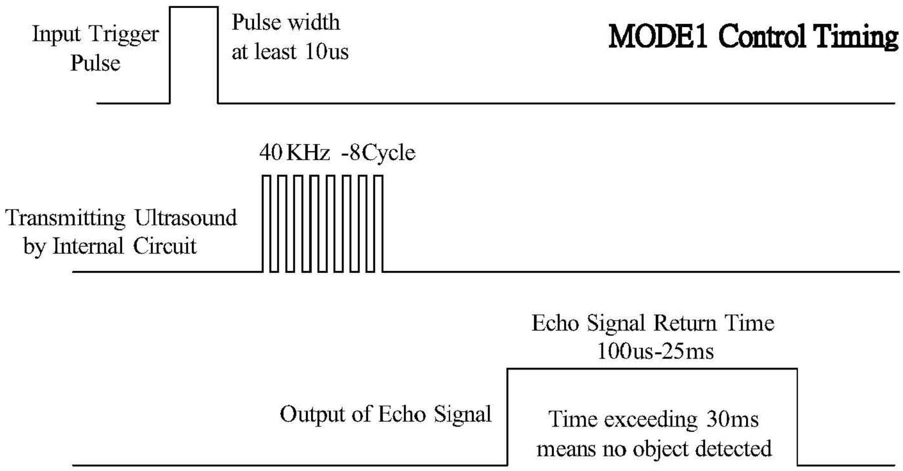

Fig. 4. Ultrasonic control timing diagram under mode 1

about 1.67cm~416cm. Conservatively, when the pulse duration exceeds 30ms, ultrasound cannot be utilized to detect the front of the obstacle. The maximum measurement error of SRF05 module is less than 3%, so the measurement performance is satisfactory.

2.2 PWM Signals of Servo Motor

Within the continuous-rotation servo motor possesses a complete position feedback control circuit. Favorable positioning results can be obtained even if the user adopts open-loop control system. Control signal for a continuous-rotation servo motor is the pulse width modulation (PWM) signal, and a variable resistor is used to calibrate the motion of servo. Since a servo motor that has just been manufactured by the factory has not been corrected, it must be calibrated before it can be used. The calibration involves applying a synthesized PWM signal, a high-state pulse of 1.5ms with a low-state voltage of 20ms, on the control terminal of the servo motor. Next, we adjust the variable resistor so that the servo unit enters a stationary state. This PWM signal is referred to as the central signal of the servo. From the manufacturer's data, in order to make continuous-rotation servo motor spin at full speed clockwise, the signal control terminal must enter a PWM signal of pulse width 1.3ms. However, to make a continuous-rotation servo motor spin at full speed counterclockwise, the pulse width must be amended to 1.7ms. Please refer to Fig. 5 for the relevant signals.

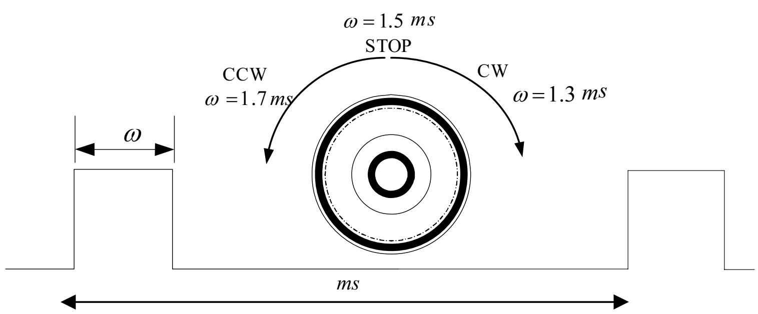

Fig. 5. Servo motor PWM drive signal

With respect to implementation, the relationship between the rotation speed of the servo motor and the width of the PWM pulse is information we are most interested in. The internal PWM generator and counter function of the embedded microcontroller ATMega162 were used to complete this experiment. To start the PWM generator, adjustable signals with a duration of 20ms and pulse widths of 1.3ms~1.7ms were sent by OC1A and OC1B pins of ATMega162, respectively to drive left and right servos, and drive rotation of wheels. With the external counter enabled, every 5s, T0 and T1 read the number of the pulse $n_x (x = 1,2)$ that was sent by the optical encoders on the left and right wheel. If the optical encoders send

N pulses per rotation of the wheels, then the servo motor speed is $2\pi n_x/5N$ (rad/s). Fig. 6 presents the related experimental results.

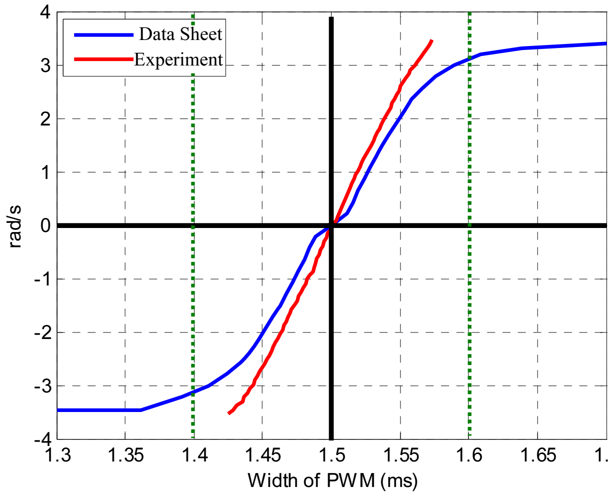

Fig. 6. Relationship between PWM pulse width and rotation speed

3 Kinematic Equation of Wheeled Mobile Robot

The problem to be attacked here is to derive the motion equation for a tri-wheeled mobile robot moving on a horizontal plane, as depicted in Fig. 7. The system may be modeled by a platform (body 4) attached by two fixed rear wheels (body 1 & 2) and one steering front wheel (body 3) with the same radius r. Let $2b$ denote the distance between the two rear wheels, and ρ_f, ρ_r be the respective distances from the mass center of the platform C_4 to that of front wheel C_3 and the center of the rear axle Q_r, l and w *be* the length and width of the body platform respectively. The contacts between the wheels and the plane are assumed to be pure rolling without side slipping.

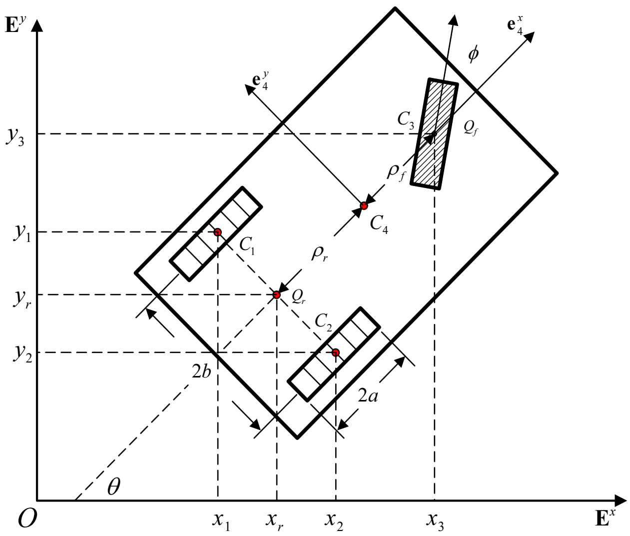

Fig. 7. The configurations of three-wheeled mobile robot

According to [12], the motion equation of the wheeled robot can be expressed as

$$\dot{x}_r = r\cos\theta v_1 + b\cos\theta v_2 \quad \textbf{(1)}$$

$$\dot{y}_r = r\sin\theta v_1 + b\sin\theta v_2 \quad \textbf{(2)}$$

$$\dot{\theta} = v_2 \quad \textbf{(3)}$$

$$\dot{\varphi}_1 = v_1 \quad \textbf{(4)}$$

$$\dot{\varphi}_2 = v_1 + (2b/r)v_2 \quad \textbf{(5)}$$

where two control inputs are defined as $v_1 = \dot{\varphi}_1$ and $v_2 = \dot{\theta}$ respectively, the actual physical significance is the rolling speed of the left wheel and the rotation speed of the wheeled robot, which can also be regarded as the linear velocity and the angular velocity of the wheeled robot.

4 Ultrasound Obstacle Avoidance Strategy Design

In this investigation, the use of ultrasonic sensing devices is combined with the wall-following method to enable robots to avoid large obstacles. From Lee [8], a wheeled robot begins from start point *S* to move along a straight line toward a target *T*, the point of encountering an obstacle is defined as the *H* point (hit point). Subsequently, the robot must adjust its azimuth posture, so that its forward direction is parallel to the edge of the obstacle, so that forward direction and maintain a safe distance *d* from the obstacle, that is, in the so-called wall-following method. In fact, Lee's article also proved that the wall-following method is an optimization scheme with finding the shortest path as the cost function. Continuing the wall-following method, as soon as the shortest distance appears between the edge of obstacle and the target, the wheeled mobile robot gets ready to deviate from the obstacle. The point of departure from the obstacle is defined as the *L* point (leave point). In principle, it is hoped the three points *H*, *L*, and *T* should be collinear, such that $\angle H_i L_i T = 180^o$ can be established, as shown in Fig. 8. Having passed point *L*, the wheeled mobile robot will be moving in the original direction of motion toward the target area. Ranging information from six ultrasonic devices that are installed on a car, shown in Fig. 9, as a judgment criterion to implement the wall-following method to avoid large obstacles and reach the target area. After the robot has entered the target area, it can effectively approach the final target point *T* using the potential field method [1], but this method requires that the location coordinates of the wheeled robot must be known in advance. Therefore, the robot must be installed with optical encoders to calculate its coordinates, or a GPS to obtain location information. The derivation and implementation in this part will be the direction of further work of this paper.

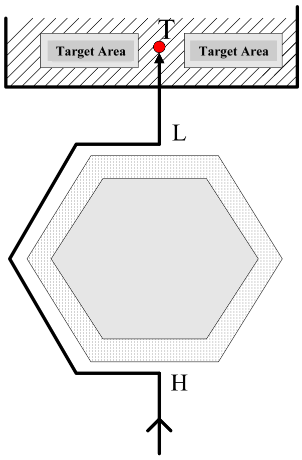

Fig. 8. Wall-following method

[Step 1] Detection of a large obstacle in front

When the wheeled robot moves forward along a straight line toward an object, its linear velocity is v_1. The angular velocity for straight forward motion is $v_2 = 0$. According to Eqs. (4) and (5), the rolling speed of the left and right wheels are obtained as $\dot{\varphi}_1 = v_1$ and $\dot{\varphi}_2 = v_1$ respectively. In order to achieve the demand on the rolling speed, servo motor of the left and right wheels are required to program the corre

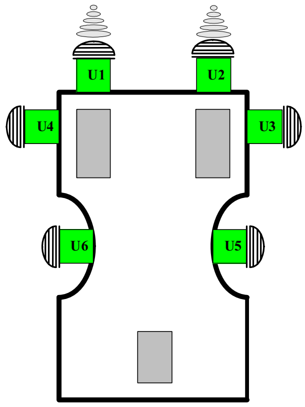

Fig. 9. Six ultrasonic devices

sponding PWM pulse width signal, refer to Fig. 6 for the relationship between rotation speed and PWM pulse width, so that the wheeled mobile robot maintains a fixed linear speed of v_1. After every t_s ms sampling time, the robot will obtain distance information between the front of wheeled robot and obstacle from ultrasonic sensors $U1$ and $U2$. If $U1$ and $U2$ detect an obstacle straight ahead, and the distance between the two is less than the safe distance safe d as previously defined, the robot will stop.

$$If \quad U1 < safe\_D \quad and \quad U2 < safe\_D \quad then \quad MR \Rightarrow Stop \tag{6}$$

That is, a signal with a 1.5ms PWM pulse width is input to the left and right wheel servo motor, forcing the robot to stop. *MR* represents the wheeled robot.

[Step 2] Adjust the robot's azimuth posture

To implement the wall-following algorithm, the posture of the robot must be adjusted to ensure that the robot moves parallel to the edge of the obstacle. Secondly, to judge whether the robot should advance forward along the right wall or left wall, the robot is assumed to advance along the left wall, and then to rotate counterclockwise to adjust the posture of its azimuth. The linear velocity of the vehicle at this time is set to v_1, the angular velocity is set to v_2, and the rolling speed of the left and right wheels are $\dot{\varphi}_1 = v_1$ and $\dot{\varphi}_2 = v_1 + (2b/r)\cdot v_2$, respectively, where v_2 determines whether the robot turns left or right. When v_2 is positive, the robot turns left; when v_2 is negative, the robot turns right. Similarly, the relationship in Fig. 6 yields the width of the PWM pulse that should be applied to the left and right wheel servo motors to make the vehicle rotation smoothly. After every sampling time, the robot reads the distance information between the side of wheeled robot and obstacle from the right ultrasonic sensor $U5$, see Fig. 9. When the rotation begins, $U5$ should not be able to detect obstacles, and distance measurement results are ∞. As rotation continues, $U5$ starts to detect obstacles, and distance measurement results will gradually become smaller, indicating that the forward direction of the robot is gradually becoming parallel to an obstacle. Once it is parallel, the $U5$ measurement results are at a minimum. Thereafter, with continuing rotation, the $U5$ measurement instead becomes larger. In other words, at each sampling time, to detect $U5$ once, the recursive measurement results should gradually become smaller. As soon as they increase, the robot stops. The forward direction of the robot at this time should be parallel to the edges of the obstacles. The algorithm is

$$\begin{aligned} & While \quad (U5_k \le U5_{k-1}) \\ & \qquad MR \Rightarrow Left \quad Turn(or \quad Right \quad Turn), \quad and \quad U5_{k-1} = U5_k \\ & end \\ & MR \Rightarrow Stop \end{aligned} \tag{7}$$

where $U5_{k-1}$ is the previous measurement value of the $U5$'s ultrasound.

[Step 3] Wall-following PD control algorithm

Only when the forward direction of the robot is parallel with the obstacles can the wall-following method be initiated. To cause the robot to maintain a safe distance d from an obstacle, and for the robot to move forward along the left wall (or the right wall), the embedded micro-controller must read the ranging information from $U3$ and $U5$ (or $U4$ and $U6$) at each sampling time, and supervise always to keep the two output of the sensors consistent, so that the front and rear of the wheeled robot remain a fixed distance from the wall. To satisfy these control requirements, a PD controller is introduced here to adjust the posture and direction of the front and rear of the robot. The linear velocity of the vehicle was set to v_1, and the angular velocity v_2 depended on the output of the PD controller. The control algorithm is as follows.

$$\begin{aligned}
&\textit{If}\ \ U5 \geq d\ \ \textit{and}\ \ U3 \geq d\ \ \textit{then}\ \ MR \Rightarrow \textit{Right Turn}. \\
&\quad e_k = d - U5,\ \ de_k = e_k - e_{k-1},\ \ v_2 = k_{p1} \times e_k + k_{d1} \times de_k. \\
&\textit{Elseif}\ \ U5 \geq d\ \ \textit{and}\ \ U3 \leq d\ \ \textit{then}\ \ MR \Rightarrow \textit{Left Turn}. \\
&\quad e_k = U5 - d,\ \ de_k = e_k - e_{k-1},\ \ v_2 = k_{p2} \times e_k + k_{d2} \times de_k. \\
&\textit{Elseif}\ \ U5 \leq d\ \ \textit{and}\ \ U3 \geq d\ \ \textit{then}\ \ MR \Rightarrow \textit{Right Turn}. \\
&\quad e_k = U5 - d,\ \ de_k = e_k - e_{k-1},\ \ v_2 = k_{p2} \times e_k + k_{d2} \times de_k. \\
&\textit{Elseif}\ \ U5 \leq d\ \ \textit{and}\ \ U3 \leq d\ \ \textit{then}\ \ MR \Rightarrow \textit{Left Turn}. \\
&\quad e_k = d - U5,\ \ de_k = e_k - e_{k-1},\ \ v_2 = k_{p1} \times e_k + k_{d1} \times de_k.
\end{aligned} \quad \textbf{(8)}$$

Basically, the relative positions of the robot and the wall can be divided into four cases. The entire robot is far from the wall, the entire robot is very close to the wall or the robot is skewed toward the wall (with the front closer to the wall than the rear, or with the front farther from the wall than the rear). For example, The $U3$ and $U5$ ultrasonic devices can detect the relative position of the robot, when the measurement signals obtained by $U3$ and $U5$ are greater than the specified safe distance d, it means the robot is turned away from the left wall. The robot must try to turn right as much as possible to approach near the wall rapidly. When the sensed distances that are obtained at $U3$ and $U5$ are both less than the safe distance d, the robot must try to turn left to stay away from the wall. If the distance measured at $U5$ exceeds the safe distance, then $U3$ is less than the safe distance, which means the vehicle is skewed (with its front close to wall and its rear away from the wall). The vehicle should turn left to prevent the front from hitting the wall. Conversely, if the distance measured at $U5$ is less than the safe distance, $U3$ is greater than the safe distance, meaning that the front is tilted outward from the wall. The entire vehicle should turn right to make the vehicle head right.

[Step 4] Toward the target area with electronic compass

The first three steps allow the wheeled mobile robot to continue the wall-following method. The last step tells the robot when it has been avoid obstacles to move toward the target area. The last step tells the robot when it should terminate the algorithm of wall-following to move toward the target area. The electronic compass receives the azimuth angle θ of the robot at each sampling time as soon as the azimuth angle changes as the robot moves. The discussion considers two cases. As the robot proceeds along the left wall, once the azimuth is within the range $-2^{\circ} \leq \theta \leq 2^{\circ}$, the wall-following algorithm stops. The robot stops and starts rotating 90° counterclockwise and moves toward the target area with angle direction of $\pi/2$. If the robot moves forward along the right wall, then once the reading of the azimuth angle is within the range $178^{\circ} \leq \theta \leq 182^{\circ}$, the robot rotates 90° clockwise and moves toward the target area.

5 Experimental Results

This study proposed the ultrasonic obstacle avoidance algorithm to find the optimized path by the wall-following method to avoid large obstacles. To verify the feasibility of the proposed obstacle avoidance strategy, Matlab7.0 was used to perform the simulation. Optimization parameters were selected based on simulation result to implement wall following algorithm. Fig. 1 shows the wheeled robot that was adopted in this work. Field measurements of the radius and tread of the left and right wheels are r = 3.3cm and $2b$ = 10.57cm, respectively. Figure 6 plots the relationship between the speed of rotation of the two sets of servo motor on the left and right wheels and the PWM pulse signal that is sent out by the embedded microcontroller. Eqs. (4) and (5) yield the relationships of linear velocity and angular velocity between rolling speed of the left and right wheels, respectively. Fig. 10 and Fig. 11 presents the simulation results of the wheeled robot as it moves continuously around a hexagonal obstacle. The radius of the obstacle is approximately 50cm, and a 10cm safety distance is maintained between the robot and the obstacle. Based on the distance information that is obtained by the ultrasonic sensors U1 to U6, the control of the wheeled robot can be divided into three steps, which are respectively the detection of the front obstacle, adjustment the posture of the azimuth angle of the robot, and execution of the wall-following algorithm. Table 1. lists the linear velocity and angular velocity in each step, the rolling speeds of the left and right wheels, and even the width of the PWM pulse that is applied by the left and right two servo motors. In the simulation, the electronic compass is used in the above three steps to enable the robot to proceed to the target area. The parameters of the PD controller are adopted as $k_{p1} = 0.5$, $k_{d1} = 0.1$, $k_{p2} = 0.2$, $k_{d2} = 0.04$, and sampling time $t_s = 2$ seconds respectively.

Table 1. The liner velocity and angular velocity in each step

Detection of obstacle in front		Adjust posture azimuth		Wall-following algorithm	
$v_1 = 1$	$v_2 = 0$	$v_1 = 0.6$	$v_2 = 0.2$	$v_1 = 1.5$	Eq.(6)
$\dot{\varphi}_1 = 1$	$\dot{\varphi}_2 = 1$	$\dot{\varphi}_1 = 0.6$	$\dot{\varphi}_2 = 1.24$	$\dot{\varphi}_1 = 1.5$	Eq.(6)
$\omega_1 = 1.52$	$\omega_2 = 1.48$	$\omega_1 = 1.51$	$\omega_2 = 0.48$	$\omega_1 = 1.53$	Fig.6
Ref. Eq.(6)		Ref. Eq.(7)		By $U3$, $U5$ (or $U4$, $U6$)	

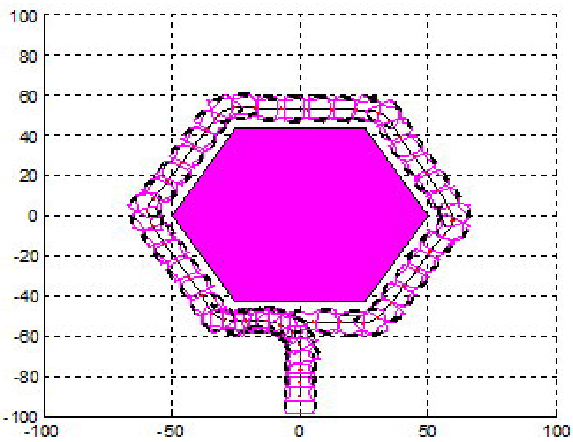

Fig. 10. Forward around the obstacle

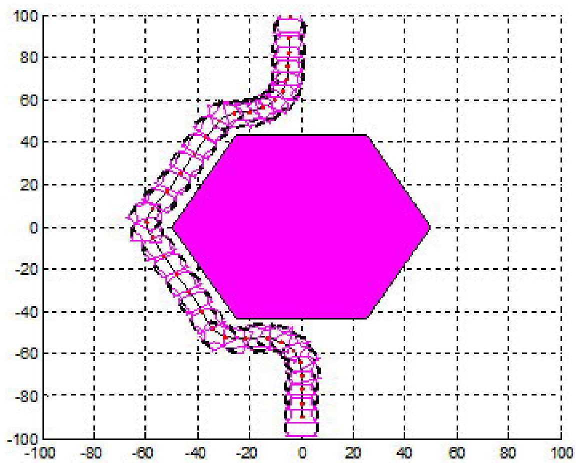

Fig. 11. Forward to the target area

Fig. 12 are photos of implementation of the wheeled robots to move forward along a hexagonal obstacle edge.

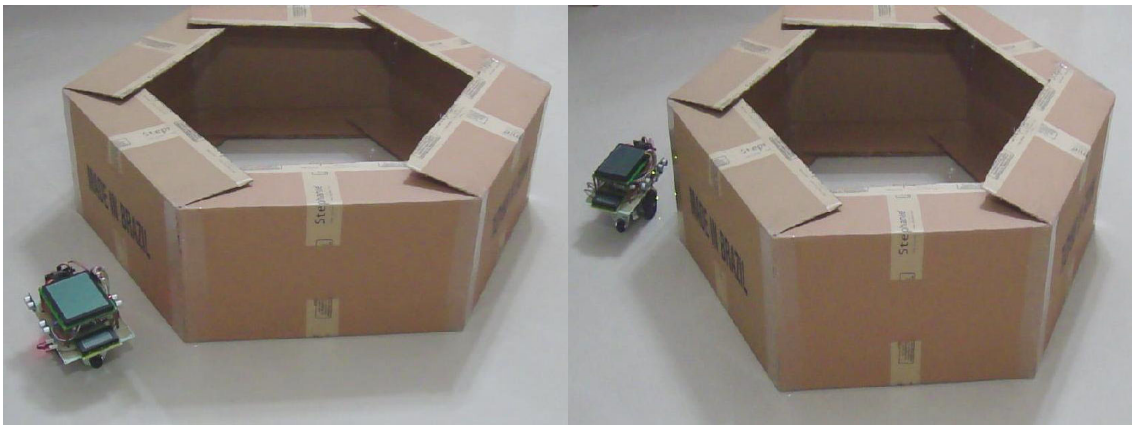

Fig. 12. Implementation of wall-following algorithm

6 Conclusions

The main contribution of this study is the establishment of a working platform for an obstacle avoidance system for small robots. The entire development, including hardware assembly, unit testing, system integration, and writing of the embedded microcontroller driving program in assembly language, were carried out systematically. Distance information, obtained by ultrasound sensors, which is suitable for point-to-point detection, is used in the wall-following method to ensure that the wheeled mobile robot avoids large obstacles. The system uses a third-generation ATMega162 chips as microcontrollers of the robot to obtain the information of six ultrasonic sensors. In the future work, small boards of embedded microprocessor ARM may replace the ATMega162 microcontrollers to deal with heavier computational loads. Furthermore, in this study, the wheeled robot eventually enters the so-called target area, but does not necessarily reach the target point, because of a lack of sensors to measure coordinate messages. Future research should also consider how to integrate optical encoders or even a global positioning system (GPS) into the system to determine the coordinates and orientation of the robot.

References

[1] S.S. Ge, Y.J. Cui, New potential functions for mobile robot path planning, IEEE Transactions on Robotics and Automation 16(2000) 615-620.

[2] E. Palma-Villalon, P. Dauchez, World representation and path planning for a mobile robot, Robotica 6(1988) 35-40.

[3] G. Paolo, G. Alessandro, A technique to analytically formulate and to solve the 2-dimensional constrained trajectory planning problem for a mobile robot, Journal of Intelligent and Robotic Systems 27(2000) 237-262.

[4] D.M. Keirsey, E. Koch, J. McKisson, A.M. Meystel, J.S.B. itchell, Algorithm of navigation for a mobile robot, IEEE International Conference on Robotics and Automation 1(1984) 574-583.

[5] E.M. Petriu, Automated guided vehicle with absolute encoded guide-path, IEEE Transactions on Robotics and Automation, 7(1991) 562-565.

[6] K. Jiang, L.D. Seneviratne, A sensor guided autonomous parking system for nonholonomic mobile robots, IEEE International Conference on Robotics and Automation 1(1999) 311-316.

[7] Y. Ando, S. Yuta, Following a wall by an autonomous mobile robot with a sonar-ring, IEEE International Conference on Robotics and Automation 4(1995) 2599-2606.

[8] H.P. Huang, P.C. Lee, Microprocessor-based control of autonomous mobile robots with obstacle avoidance, Proceedings of the 30th Conference on Decision and Control 1(1991) 678-683.

[9] R.A. Hogle, P.P. Bonissone, A fuzzy algorithm for path selection in autonomous vehicle navigation, in: Proc. of the 23rd Conference on Decision and Control, 1984.

[10] Y. Han, H. Hahn, Localization and classification of target surfaces using two pairs of ultrasonic sensors, Elsevier Science on Robots and Autonomous Systems 1(2000) 31-41.

[11] D. Silver, D. Morales, I. Rekleitis, B. Lisien, H. Choset, Arc carving: obtaining accurate, low latency maps from ultrasonic range sensors, IEEE International Conference on Robotics and Automation 2(2004) 1554-1561.

[12] P.S. Tsai, Modeling and control for wheeled mobile robots with nonholonomic constraints, [disseration] National Taiwan University, 2006.